Research Article

Identification of Inputs to Olivocochlear Neurons Using Transneuronal Labeling with Pseudorabies Virus (PRV)

M. Christian Brown,[1,2] Sudeep Mukerji,[1] Marie Drottar,[1] Alanna M. Windsor,[1] and Daniel J. Lee[1,2]

[1]*Eaton-Peabody Laboratory, Massachusetts Eye and Ear Infirmary, 243 Charles St, Boston, MA 02114, USA*
[2]*Department of Otology and Laryngology, Harvard Medical School, Boston, MA 02114, USA*

ABSTRACT

Olivocochlear (OC) neurons respond to sound and provide descending input that controls processing in the cochlea. The identities of neurons in the pathways providing inputs to OC neurons are incompletely understood. To explore these pathways, the retrograde transneuronal tracer pseudorabies virus (Bartha strain, expressing green fluorescent protein) was used to label OC neurons and their inputs in guinea pigs. Labeling of OC neurons began 1 day after injection into the cochlea. On day 2 (and for longer survival times), transneuronal labeling spread to the cochlear nucleus, inferior colliculus, and other brainstem areas. There was a correlation between the numbers of these transneuronally labeled neurons and the number of labeled medial (M) OC neurons, suggesting that the spread of labeling proceeds mainly via synapses on MOC neurons. In the cochlear nucleus, the transneuronally labeled neurons were multipolar cells including the subtype known as planar cells. In the central nucleus of the inferior colliculus, transneuronally labeled neurons were of two principal types: neurons with disc-shaped dendritic fields and neurons with dendrites in a stellate pattern. Transneuronal labeling was also observed in pyramidal cells in the auditory cortex and in centers not typically associated with the auditory pathway such as the pontine reticular formation, subcoerulean nucleus, and the pontine dorsal raphe. These data provide information on the identity of neurons providing input to OC neurons, which are located in auditory as well as non-auditory centers.

Keywords: superior olive, cochlear nucleus, inferior colliculus, reflex pathway, reticular formation

Correspondence to: M. Christian Brown · Eaton-Peabody Laboratory · Massachusetts Eye and Ear Infirmary · 243 Charles St, Boston, MA 02114, USA
Telephone: +1-617-5733875; fax: +1-617-7204408: email: Chris_Brown@meei.harvard.edu

INTRODUCTION

Olivocochlear (OC) neurons provide an efferent pathway by which the brain can exert control over the cochlea. These efferent neurons have cell bodies in the brainstem's superior olivary complex and consist of two subgroups: (1) medial (M) OC neurons, which are large neurons located mainly in the ventral nucleus of the trapezoid body, and (2) lateral (L) OC neurons, which are smaller neurons located in and on the margins of the lateral superior olive. Neurons of the MOC subgroup respond to sound as part of a reflex, which functions to reduce the effects of background noise and to protect the cochlea from acoustic overexposure (reviewed by Ryugo et al. 2011). The function of LOC neurons is more obscure, but they may balance the neural sensitivity of the auditory nerves on the left and right sides (Darrow et al. 2006).

Reflexive inputs from the cochlear nucleus (CN) drive the MOC neuron's response to sound (Warr 1969; Thompson et al. 1991; Liberman and Guinan 1998; Ye et al. 2000; Brown et al. 2003). LOC neurons also receive CN inputs but their sound-evoked responses have not been determined. In addition to reflexive inputs, OC neurons also receive descending inputs from higher levels of the auditory pathway. These inputs, especially to MOC neurons, come from

the inferior colliculus (IC) (Faye-Lund 1986; Thompson and Thompson 1993; Vetter et al. 1993) and the auditory cortex (Mulders and Robertson 2000a). Finally, the OC neurons receive input from centers not typically associated with the auditory pathway, such as those positive for noradrenaline (Mulders and Robertson 2005a) and serotonin (Thompson and Thompson 1995). The role of these other inputs is unclear, but they may modulate the reflexive input or mediate functions related to attention (Delano et al. 2007).

For the most part, the OC inputs listed above have been documented by the use of conventional neuronal tracers. Typically, one tracer is used to retrogradely label the OC neurons and a second tracer is used to anterogradely label the suspected input. Usually, this approach has the disadvantage of large injection sites. For example, injections into the posteroventral cochlear nucleus (PVCN) demonstrate projections to MOC neurons (Thompson and Thompson 1991), but the reaction product at the injection site obscures the identity of the cells forming the projections. The present approach avoids this problem with the use of transneuronal labeling via the Bartha strain of pseudorabies virus (PRV) (Enquist and Card 2003; Ekstrand et al. 2008). This virus is picked up by axon terminals at the injection site and transported back to neuronal cell bodies. There, the virus replicates and is amplified. It then crosses to nerve terminals synapsing on the cells and in turn transports back to the cell bodies providing those inputs, which are remote from the injection site and not obscured by it. Transneuronal labeling has been used to study the OC pathways in the pioneering work of Horvath et al. (2003). After injections of PRV-Bartha into the cochlea, labeling was first observed in the OC neurons and, at later times, within neurons in other locations. Transneuronally labeled neurons were found in the CN, IC, auditory cortex, and in centers not typically associated with the auditory pathway such as the subcoerulean nucleus and pontine dorsal raphe (Horvath et al. 2003). PRV-Bartha is ideal for OC labeling because it is transported exclusively in the retrograde direction (O'Donnell et al. 1997; Card et al. 1998), thus avoiding a complication of anterograde labeling of auditory nerve projections to the CN (Horvath et al. 2003).

We apply transneuronal labeling to address several important questions about the OC system. First, since cochlear injections of PRV label both MOC and LOC neurons, it is not clear whether transneuronal labeling in CN and IC proceeds via one or the other or both of these populations. We found case-by-case variability in labeling of MOC vs. LOC neurons. An overall analysis of these injections demonstrated a greater correlation between the amount of transneuronal labeling and MOC labeling, compared to LOC labeling, suggesting that much, but not all, transneuronal labeling proceeds via MOC neurons.

Secondly, we seek to identify the types of cells that are transneuronally labeled and thus provide the OC inputs. Both the CN and the IC contain major classes of neurons, each having its own unique anatomy, physiology, and projections (Osen 1969; Oliver and Morest 1984). The CN is particularly interesting because it plays a critically important intermediate stage in the MOC reflex pathway (Liberman and Guinan 1998; de Venecia et al. 2005). CN transneuronal labeling is found in multipolar cells (Horvath et al. 2003), but the labeled subtype within this heterogeneous class (reviewed by Doucet and Ryugo 2006) was not identified. Recent work using conventional tracers suggests that one class, planar multipolar cells, projects to MOC neurons (Darrow et al. 2012), and we examine here whether they and other subtypes are transneuronally labeled. We also examine whether the two types of IC neurons, cells with disc-shaped dendritic fields and cells of stellate shape, are transneuronally labeled. Finally, we confirm the numerous types of "non-auditory" transneuronally labeled neurons reported by Horvath et al. (2003). It is not clear how these inputs participate in the OC reflex to sound, and information here may help us better understand the role of OC neurons in the greater realm that includes auditory and non-auditory processes.

MATERIALS AND METHODS

All surgical procedures and techniques for anesthesia comply with NIH, Harvard Medical School Biosafety Committee, and Massachusetts Eye and Ear Infirmary guidelines and were performed in a Biosafety Level 2 suite. Adult guinea pigs (500 to 800 g) were anesthetized with Nembutal (19 mg/kg, i.p.), droperidol (10 mg/kg, i.m.), and fentanyl (0.2 mg/kg, i.m.). A post-auricular surgical approach was performed and the bulla opened to visualize the basal turn of the left cochlea. The round window membrane was torn and the stapes footplate was displaced. PRV 152, which is isogenic with PRV-Bartha but contains an EGFP expression cassette cloned into the middle of the PRV gG gene and grown in pig kidney cells (PK15) as described previously (Smith et al. 2000; Pickard et al. 2002), was provided by Dr. L.W. Enquist (Princeton University). The virus was stored at –80 °C and frozen aliquots were quickly thawed to 37 °C in a water bath, ultrasonicated (Misonix, Inc.), and centrifuged before inoculation. Aliquots contained 10^9 plaque-forming units per milliliter. Injections of PRV were made through the round window in steps of 2 µl with a 10-µl Hamilton syringe. Fluid was wicked from the oval window between steps. An average total of 15 µl (range of 5–30 µl) was injected. Dental pledgets were used to

minimize secondary spread into surrounding structures of the middle ear. Following surgical closure of the wound and recovery, the animals underwent a 1–5-day survival time in the Biosafety Level 2 suite.

The animals were then re-anesthetized and perfused through the vascular system with saline and then with 4 % paraformaldehyde in 0.1 M phosphate buffer (pH 7.3). Dissected brainstems or cortex pieces were immersion-fixed for 2–4 h and then washed in PBS. For most animals, the brainstem was then immersed in 30 % sucrose overnight and then sectioned (80 μm) on a freezing microtome. Brainstem sections were collected that included the CN, superior olivary complex, and the IC. In some cases, pieces of the temporal cortex were embedded in a gelatin albumin mixture and sectioned (also at 80 μm) on a Vibratome. In two animals, the injected cochleas were decalcified and then embedded according to the method of Hurley et al. (2003) and sections cut on a freezing microtome. In a few animals, sections were examined in the fluorescent microscope without further processing. In most animals, sections were blocked for 1 h with 10 % NGS/1 % BSA, followed by incubation with 1:500 primary antibody anti-GFP rabbit IgG fraction (Invitrogen Inc.) for 2 days at 4 °C to penetrate to the interior of the section. The sections were washed extensively in PBS and incubated with 1:500 biotinylated goat anti-rabbit secondary antibody (Invitrogen Inc.) for 2 h, washed again, and then incubated with an ABC kit and finally with diaminobenzidine. Sections were mounted and coverslipped for viewing in the light microscope. Although the reaction product is formed to GFP, we will describe neurons with reaction product as "PRV-labeled."

A total of 33 guinea pigs received cochlear injections and underwent brainstem tissue processing. Six of the cases had no labeled OC neurons and no labeling elsewhere in the brainstem. Twenty-seven cases had labeled OC neurons (Table 1). The cortices were processed in 13 of these animals (see Fig. 2 legend). Two additional guinea pigs received control injections of PRV into the middle ear space (instead of the cochlea), and after a 3-day survival time, there were no labeled neurons in the brainstem. Three other guinea pigs received cochlear injections of 30 % horseradish peroxidase in saline. After a 24-h survival time, they were perfused and sectioned as described above. Sections were reacted with tetramethylbenzidine (Mesulam 1982) and counterstained with neutral red.

Labeled neurons were counted only if they contained dark reaction product in comparison to background. From plots of the numbers of labeled neurons in different brainstem centers vs. the number of labeled OC neurons, linear fits and linear (Pearson) correlation coefficients (R) were computed using Kaleidagraph software. Correlation coefficients near 1 represent a linear relationship in which the variables are highly correlated (Pagano and Gauvreau 2000); the relationships were considered significant if the P values were ≤0.05. Internal subdivisions of the nuclei were delineated as described in previous works on the rodent CN (Hackney et al. 1990) and the IC (Oliver and Morest 1984; Loftus et al. 2008). Micrographs were obtained with a compound microscope fitted with a digital camera and were not further processed.

RESULTS

PRV labeling of OC neurons

Following injections of PRV into the cochlea, labeled neurons were found in the superior olivary complex. Labeled neurons of small size were found within the lateral superior olive (LSO, Fig. 1A), with a few of larger size on its margins. These neurons were grouped together as LOC neurons. MOC neurons were found in the ventral nucleus of the trapezoid body (VNTB, Fig. 1B) and dorso-medial periolivary nucleus (DMPO). These neurons were well filled with reaction product that often extended into their dendrites. Their appearance was generally similar to such neurons when they were labeled by conventional neural tracers such as horseradish peroxidase (HRP) (Strutz and Bielenberg 1984). One difference was that sometimes in the vicinity of PRV-labeled neurons, there were "cloudy" extracellular deposits of reaction product (Fig. 1A) and labeled profiles ("blebs," Fig. 1B) that may signify cells in the late stages of cytopathic changes from PRV infection (Billig et al. 2007). MOC somata major and minor axis diameters (average 25.4×15.4 μm, SD 5.4×3.3 μm, for 51 neurons) were significantly larger than LOC somata from within the LSO (average 15.9×10.5 μm, SD 3.1× 2.6 μm, for 28 neurons). The few neurons located on the LSO margins (LOC "shell neurons," Vetter and Mugnaini 1992) were large (average 28.9×11.9 μm, SD 5.2×2.2 μm, for four neurons). Some MOC neurons and LOC shell neurons had dendrites with visible spines (Mulders and Robertson 2000b; Benson and Brown 2006; Brown et al. 2013a). Axonal labeling was uncommon, but several cases had a few OC axons projecting dorsalward in the brainstem.

The pattern of PRV labeling changed with survival time after injection (Fig. 2, Table 1). At 1 day, the two cases had solely OC labeling without any labeling in the CN (Fig. 2A). This observation suggests that PRV labeling is via the retrograde direction, rather than via auditory nerve fibers in the anterograde direction. Also in support of this view, no labeling was seen in auditory nerve fibers entering the cochlear nucleus, and labeling was not seen in spiral ganglion cells in the two cochleas that were processed (both 2-day

TABLE 1

PRV labeling data

			Number of PRV-labeled neurons[a]			
GP	PRV (μl)	Survival time (days)	LOC	MOC	CN	IC
29	25	1	1	0	0	0
30	25	1	0	4	0	
1	25	2	5	7	0	0
2	20	2	1	0	0	0
10	20	2	3	4	11	7
15	10	2	1	1	0	0
16	10	2	6	43	1	0
17	8	2	51	0	0	0
19	10	2	4	0	0	0
11	20	2	1	1	0	0
26	25	3	7	10	33	6
2008_2	6	3	4	4	8	45
8	5	3	63	33	59	1
12	20	3	114	214	175	
14	30	3	255	384	283	264
21	10	3	7	6	2	
22	10	3	48	10	62	31
24	18	3	39	21	92	3
28	25	3	134	172	396	35
2008_1	24	3	72	137	110	127
7	5	4	39	233	185	526
5[b]	5	4	2	65	51	35
6	5	4	31	466	500	1,384
2008_6	18	4	6	3	20	
2008_7[b]	12	4	28	8	5	2
3[b]	20	5	42	220	228	814
4	20	5	46	96	63	60

The four cases with no entry in the IC column had incomplete sections

[a] Counts are of bilateral labeling

[b] Cases illustrated in Figure 3 (B, C, and A, respectively)

survival times). At later times, the numbers of OC neurons (Fig. 2B) increased and then formed a plateau.

In the plateau, OC labeling averages 177.6 neurons per animal (range 8–639, SD 185.3, $n=17$ animals with
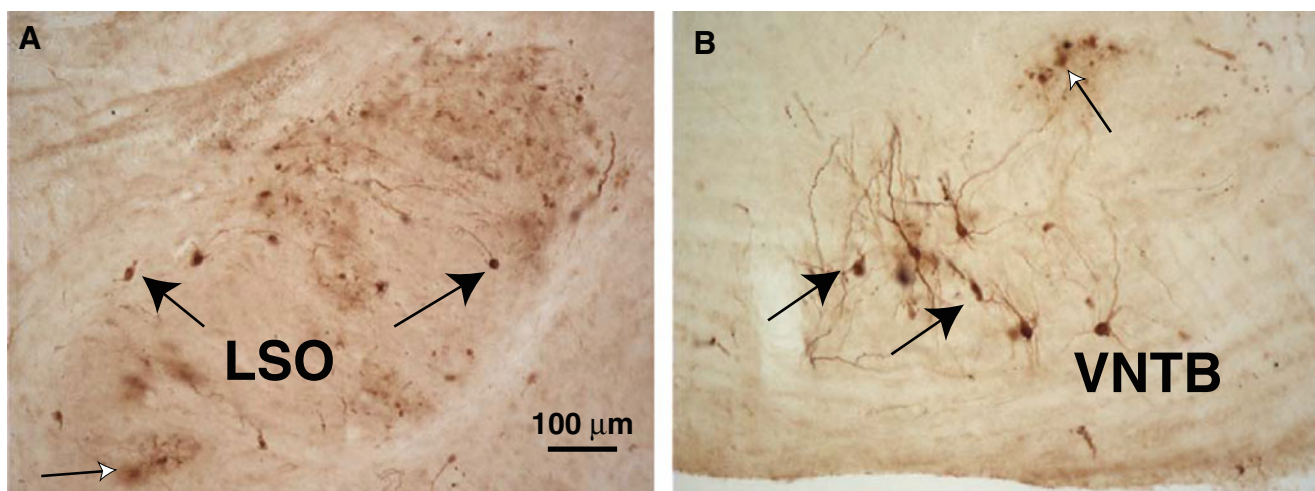

FIG. 1. Photomicrographs of PRV-labeled neurons. **A** Labeled LOC neurons (*black arrows*) in the lateral limb of the lateral superior olive (LSO) on the side ipsilateral to the injected cochlea after a 3-day survival time. "Cloudy" areas of reaction product (*white arrow*) were sometimes observed in areas of PRV labeling (see text). This section is at the mid-point of the LSO's rostro-caudal extent. **B** Labeled MOC neurons (*black arrows*) in the ventral nucleus of the trapezoid body (VNTB) on the side contralateral to the injected cochlea, in an animal that survived for 3 days after the injection (a different case from **A**). A labeled group of "blebs" is indicated by a *white arrow* (see text). This section is from the caudal VNTB, near the caudal tip of the LSO.

FIG. 2. PRV labeling as a function of post-injection survival time. **A** Percentage of cases with labeling in the indicated centers (*OC* olivocochlear neurons, *CN* cochlear nucleus, *NLL* nuclei of the lateral lemniscus, *IC* inferior colliculus, *Retic* reticular formation of the brainstem, *Raphe* brainstem dorsal raphe, *LC* locus subcoeruleus, *AC* auditory cortex). **B** Number of labeled neurons as a function of survival time after injection (color coding as in panel **A**). Average number per brain represents counts of bilateral labeling following PRV injection into one cochlea. OC counts are combined LOC and MOC subgroups. *Error bars* show one standard error of the mean. **C** Number of labeled neurons divided by the number of MOC neurons. The number of animals included were as follows: 1 day: two brainstems; 2 days: eight brainstems, one cortex; 3 days: nine to ten brainstems, seven cortices; 4 days: three to five brainstems, three cortices; 5 days: two brainstems, two cortices. Control represents two animals injected into the middle ear (survival time, 3 days) in which there was no labeling. For survival times of 2–5 days, only cases with labeled OC neurons were used. Control counts are assumed to be zero for AC.

survival times 3–5 days). MOC neurons outnumbered LOC neurons (average 122.5, SD 141.8 vs. 55.1, SD 63.5, survival times 3–5 days) and there was large variability from case to case (Table 1). There was no clear relationship between the injection volume and the number of OC neurons labeled or the relative proportions of labeled MOC and LOC neurons (data not shown). In contrast, HRP labeling yields an average of 1,313 neurons per animal (range 729–1997, SD 572.1, $n=3$ animals) even though the injection methods were similar. Both tracers labeled MOC and LOC neurons bilaterally in the brainstem, with MOC neurons primarily contralateral and LOC neurons primarily ipsilateral. For MOC neurons, 54.7 % of the PRV-labeled neurons were on the brainstem side contralateral to the injection (25 injections) and 64.7 % of the HRP-labeled neurons were contralateral. For LOC neurons, 90.2 % of the PRV-labeled neurons were ipsilateral and 94.6 % of the HRP-labeled neurons were ipsilateral.

Apparent retrograde labeling of a few neurons that were not olivocochlear was observed but infrequently. In three cases, one of which was a 2-day survival time, there was scattered labeling of a few vestibular efferent neurons (bilaterally, near the facial genu and/or in the pontine reticular formation, Strutz 1982). One of these PRV cases had a few labeled neurons in the ipsilateral medial vestibular nucleus, but their other patterns of labeling were not different. Our HRP-labeled cases also had retrograde labeling of vestibular efferents, and their numbers were usually greater than for PRV labeling. In four other PRV-injected cases, there were small numbers of labeled neurons in the facial motor nucleus on the ipsilateral side, presumably via spread of the virus to the facial nerve that courses adjacent to the middle ear. The cases were distributed across the survival times used. Since they did not differ from other cases in the labeling pattern seen elsewhere, they were included in our database. One case had labeling in the vicinity of the inferior salivatory nucleus (Contreras et al. 1980; Spangler et al. 1982).
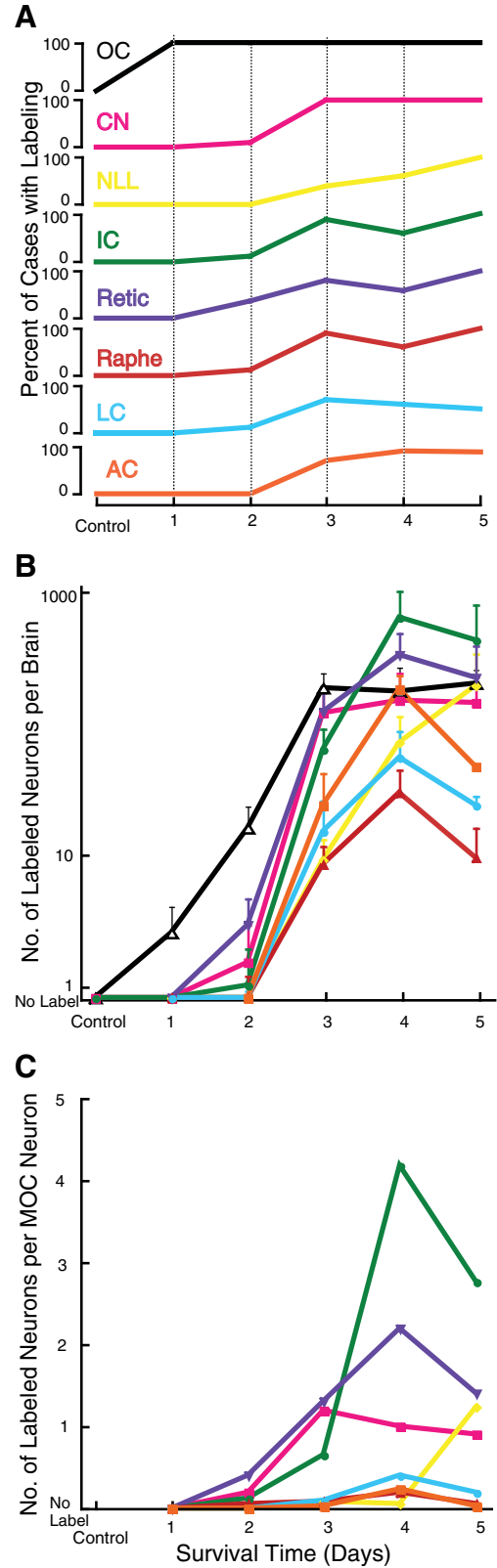
Spread of PRV labeling

PRV labeling spread to other brainstem areas for survival times of several days (Fig. 2A, B, Table 1), and this time lag after OC labeling is a key element to the

idea that this labeling is transneuronal. A comparison of the number of labeled OC neurons and the number of transneuronally labeled neurons in other centers is shown in Figure 2B. Labeling of OC neurons, which began on day 1, increased and formed a plateau that began on day 3. Labeling in the brainstem reticular formation, the CN, and the IC lagged that for OC neurons, beginning on day 2, increasing at day 3, and forming a plateau in the reticular formation and CN on day 3 and in the IC on day 4. The plateau number of labeled CN neurons per animal was about 150, about the same as for MOC neurons, and the plateau number of IC neurons per animal was between 400 and 700. The other brainstem centers and auditory cortex had transneuronal labeling beginning at 3 days, 1 day later than the reticular formation, the CN, and the IC.

Figure 3A illustrates the pattern of labeling in a case with both MOC and LOC neurons and abundant transneuronal labeling in CN and IC. Within the CN, the most labeling was in the anteroventral (AVCN) subdivision, which is the largest subdivision, with less labeling in the PVCN and the dorsal subdivision (DCN). Overall for all of our dataset, in which a total of 2,062 labeled CN neurons were found, AVCN had the largest number (56.5 %), followed by the PVCN (27.5 %) and DCN had the fewest (16 %). The labeling in the different CN subdivisions had the same time course (data not shown). Labeling in the CN was heaviest on the injected side (Fig. 3A, and overall for the dataset, 78.5 % of CN labeling was ipsilateral). In the IC, most of the transneuronally labeled neurons were within the central nucleus and the dorsal cortex and a few were in the lateral cortex. IC labeling was somewhat greater on the side contralateral to the injection (Fig. 3A, 56.7 % on the contralateral side for a total of 3,332 neurons of all cases).

In the nuclei of the lateral lemniscus, there were about twice as many labeled neurons on the contralateral side as the ipsilateral side. For cases like this one, where both LOC and MOC neurons are labeled, it is not possible to determine the degree of transneuronal labeling that occurs via one or another of these subgroups.

Some of our injection cases had fewer numbers of labeled neurons and unequal labeling of the two subgroups of OC neurons. One case in which there was predominantly MOC labeling (Fig. 3B) also had transneuronally labeled neurons in the CN and IC (see Table 1 for counts). This case illustrates that abundant transneuronal labeling can occur when mostly MOC neurons are labeled. Conversely, there were several animals (one illustrated in Fig. 3C), in which there were few MOC neurons but modest numbers of LOC neurons, and these cases had almost no transneuronal labeling in the CN or IC. These cases suggest that transneuronal labeling occurs less frequently via LOC neurons. The relationship between the numbers of transneuronally labeled neurons in the CN and IC vs. the fraction of OC labeling that is MOC labeling is given in Figure 4. The data illustrate that when the ratio is greater than 0.5 (there are more labeled MOC neurons than LOC neurons), there is usually a large amount of transneuronal labeling.

Overall, for all cases, the R values for the correlation of labeled MOC neurons and labeled neurons in the CN and IC were significant (Fig. 5A, see correlation coefficient given on plot and best-fit equations in the legend). When the CN labeling was segregated by subdivision, the correlation between MOC labeling and PVCN labeling was significant ($R=0.91$, $P=0.0000004$), and for AVCN labeling, it was also significant ($R=0.86$, $P=0.00001$). The neural pathway
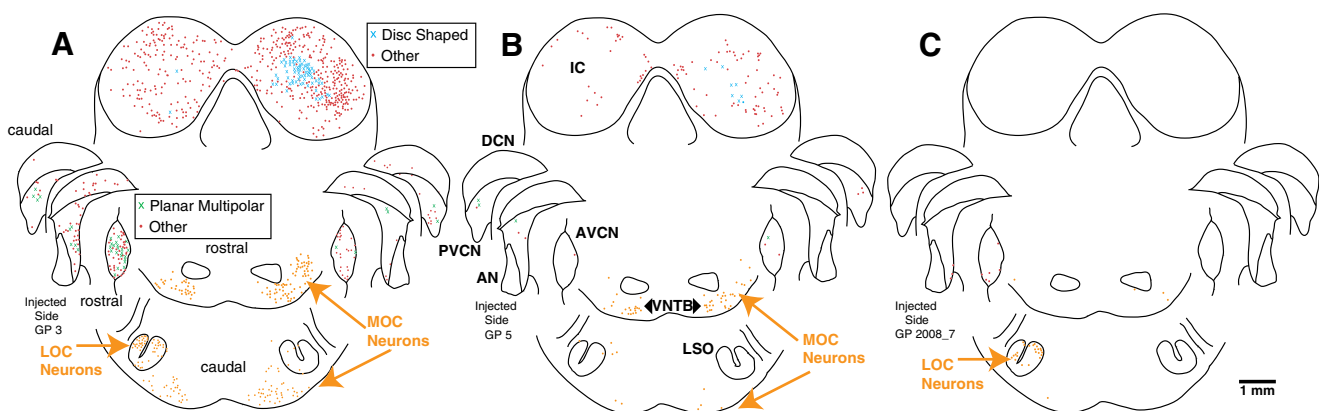

FIG. 3. Atlases of PRV labeling in the brainstems of three animals. The first injection case (**A**) had many labeled OC neurons and abundant transneuronal labeling in the CN and IC (see Table 1 for counts). Most of the CN labeling was in the AVCN. The second injection case (**B**) had a moderate amount of MOC labeling, almost no LOC labeling, and some CN and IC transneuronal labeling. In contrast, the third injection case (**C**) had almost no labeling of MOC neurons, a moderate amount of LOC labeling, and minimal transneuronal labeling. Most of the CN labeling in this case was in rostral AVCN. *Each symbol* represents a single labeled neuron (see key for cell type, where "Other" means that the neuron could not be identified). The atlas drawings divide CN labeling into caudal, middle, and rostral portions. The superior olivary complex labeling at the bottom of the figure is divided into caudal labeling (in and around the LSO) and more rostral labeling. Survival time was 5 days for **A** and 4 days for **B** and **C**.
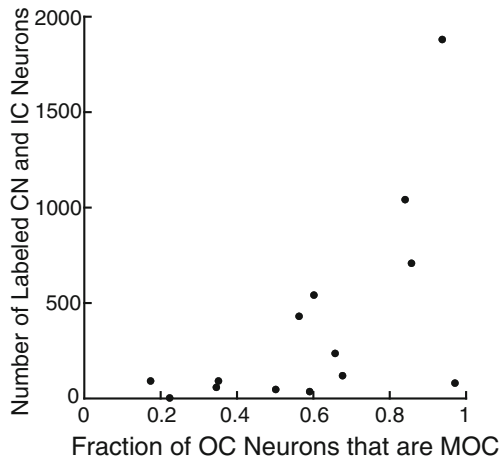
FIG. 4. Relationship between the number of transneuronally labeled neurons in the CN and IC and the fraction of OC labeling that was MOC, for cases with survival times of 3–5 days. Three cases with incomplete sections of IC (Table 1) were not used.

of the MOC reflex predicts that the MOC neurons receive dominant inputs from the CN on the opposite side (Liberman and Guinan 1998). Correlation coefficients were significant for MOC labeling on the side contralateral to the injection and CN labeling on the opposite side and vice versa ($R=0.75$, $P=0.0005$ and $R=0.70$, $P=0.0018$, respectively). Although the overall correlation of labeled LOC neurons and labeling in the CN was not significant (see legends of Figs. 5B and 6B), there was a relationship between LOC labeling and a few cases with labeling in the rostral and ventral parts of the ipsilateral AVCN. For example, Figure 3C illustrates a case in which there was OC labeling in LOC neurons and in which there was labeling in the rostral AVCN on the ipsilateral side (see also Fig. 7B). For all cases combined, there was a weak correlation ($R=0.65$, $P=0.008$) between labeling in LOC neurons and labeling in the rostral half of the ipsilateral AVCN.

In the IC, the number of labeled neurons was also correlated with the number of labeled MOC neurons (Fig. 6A). Other studies (Faye-Lund 1986; Thompson and Thompson 1993; Vetter et al. 1993; Groff and Libeman 2003) suggest that descending projections

from the IC travel to MOC neurons on the same side of the brain. The correlation between contralaterally located MOC neurons and contralaterally located IC neurons was strong ($R=0.85$, $P=0.0001$), but there was also a high correlation with ipsilaterally located IC neurons ($R=0.94$, $P=0.0000006$). The correlations between ipsilaterally located MOC neurons and ipsilaterally located IC neurons ($R=0.78$, $P=0.001$) and contralaterally located IC neurons ($R=0.70$, $P=0.005$) were lower but still significant. Given the correlations with MOC labeling, we normalized the numbers of transneuronally labeled neurons by the numbers of labeled MOC neurons (Fig. 2C). These normalized numbers can be interpreted as the "productivity" of transneuronal labeling: numbers greater than one indicate more transneuronally labeled neurons compared to MOC neurons, and those less than one indicate fewer. The most productive center was the IC, where, for peak survival times, the number or transneuronally labeled neurons was about four times the number of MOC neurons. The reticular formation and CN were the next most productive. The auditory cortex was the least productive.

Transneuronal labeling is in CN multipolar cells

Examples of labeled CN neurons are seen in the micrographs of Figure 7. The reaction product within many of these neurons and their processes was good enough for them to be identified. The classified neurons were almost all multipolar neurons (Fig. 7) because they have three or more dendrites protruding at widely divergent angles from their somata (Hackney et al. 1990). We classified the 1,200 neurons from the ventral cochlear nuclei on both sides in four animals with the heaviest labeling. Of these neurons, 50.0 % were multipolar. Many others (49.1 %) had a similar appearance although they could not be definitively classified, either because their dendrites were not available in the section that contained their cell bodies or because of light labeling of their dendrites. The remaining small numbers of neurons were bushy
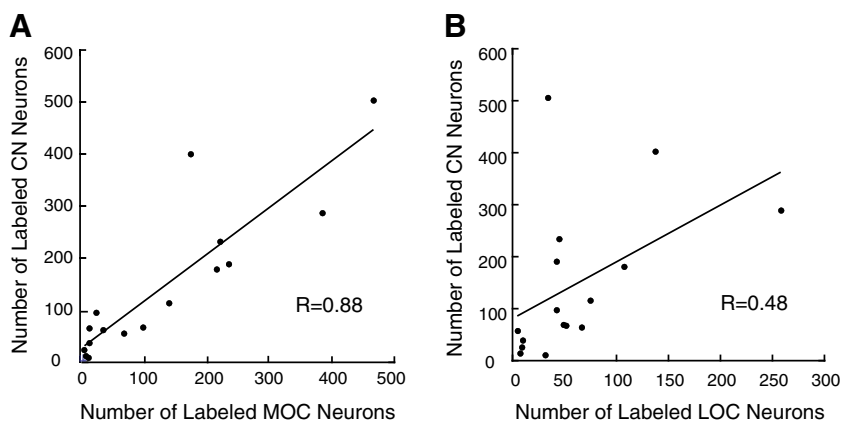

FIG. 5. Relationship between the numbers of transneuronally labeled CN neurons and the number of labeled MOC neurons (**A**) or LOC neurons (**B**). Data are from injection cases with survival times of 3–5 days. Correlation coefficients are given on the plots and are significant for the MOC relationship ($P=0.000003$) but not for the LOC relationship ($P=0.051$).
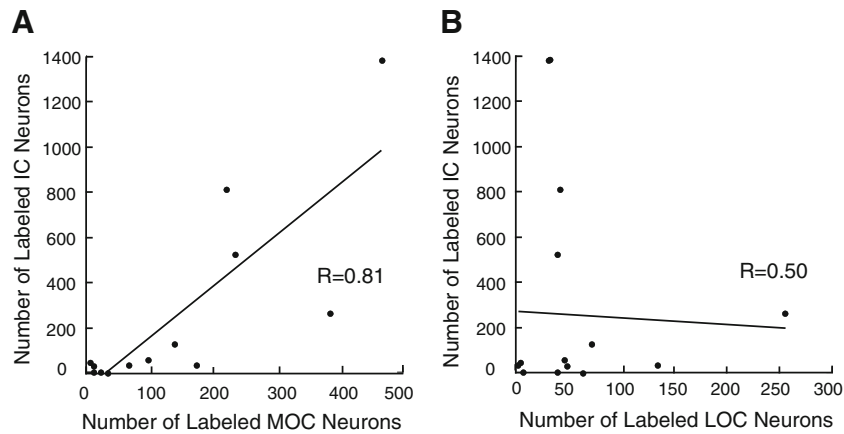
FIG. 6. Relationship between the numbers of transneuronally labeled IC neurons and the number of labeled MOC neurons (**A**) or LOC neurons (**B**). Data are from injection cases with survival times of 3–5 days. Correlation coefficients are given on the plots and are significant for the MOC relationship (*P*=0.0006) but not for the LOC relationship (*P*=0.069).

(0.5 %) and octopus cells (0.4 %) as defined by Hackney et al. (1990). Almost all labeled neurons were located in the core of the CN rather than around its edges. In particular, there was almost no labeling in the edge region known as the superficial layer of granule cells (Fig. 8, sgl) or in the cap of small cells at the dorsal-most edge of AVCN just below this layer. In the DCN, the small amount of labeling was limited to multipolar and fusiform cells and a few giant and cartwheel cells.

The predominant subtype of transneuronally labeled multipolar cell had a medium-sized cell body and dendrites with an orientation flattened in the isofrequency plane (Fig. 7, black arrows). Cells of this

morphology are described by Doucet and Ryugo (1997, 2006) as "planar cells." The somata of these cells averaged 214.6 µm² in area (SD 54.2 µm², *n*=39 cells, average major axis 19.9 µm and average minor axis 13.0 µm). Their dendrites extended up to 150 µm from the soma. Our counts indicate that 64.6 % of the neurons classified as multipolar neurons were planar cells. The remaining multipolar neurons (35.4 %) had dendrites radiating from the cell body in diverse directions (Fig. 7A, white arrow). These somata were also medium in size (average area 205.3 µm², SD 62.1 µm², not significantly different from planar cells). We did not observe labeling of the largest "radiate" multipolar cells (Doucet and Ryugo 1997). The distribution of planar
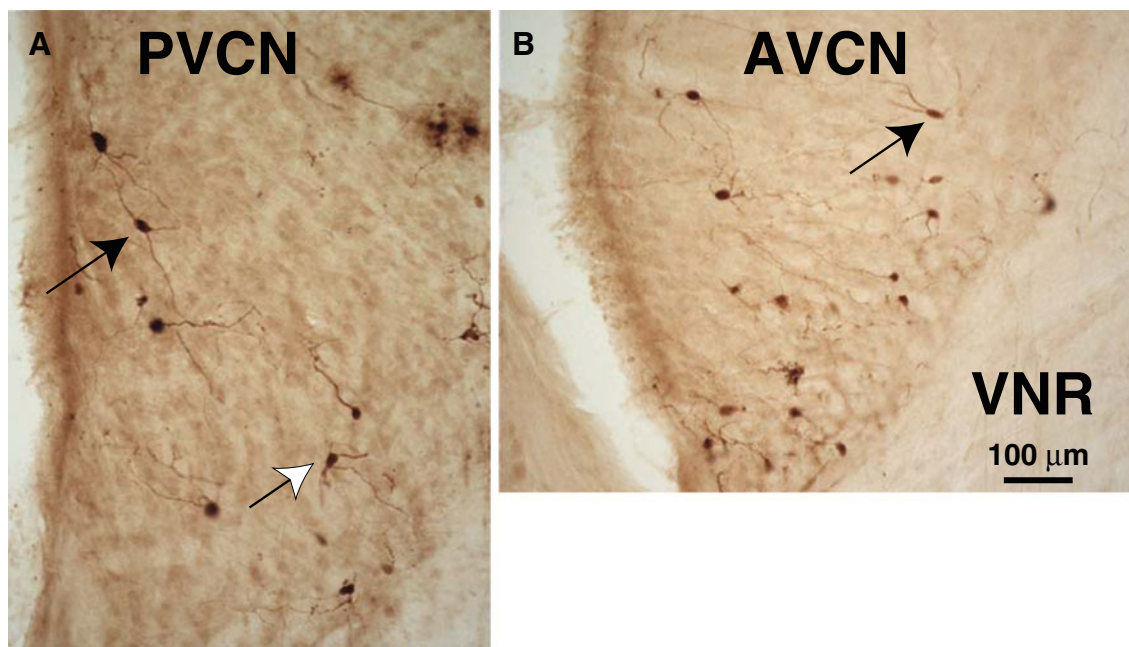

FIG. 7. Photomicrographs of PRV-labeled multipolar neurons in PVCN (**A**) and AVCN (**B**). Planar multipolar cells (*black arrows*) have long dendrites mostly contained in a single plane and cell bodies of medium size (see text for measurements). Other multipolar cells have more radiating dendrites (*white arrow*). Both **A** and **B** are from the CN ipsilateral to the injection and both had a 3-day survival time. *VNR* vestibular nerve root. These sections are from a point about midway in the total rostro-caudal extent of the PVCN and AVCN.
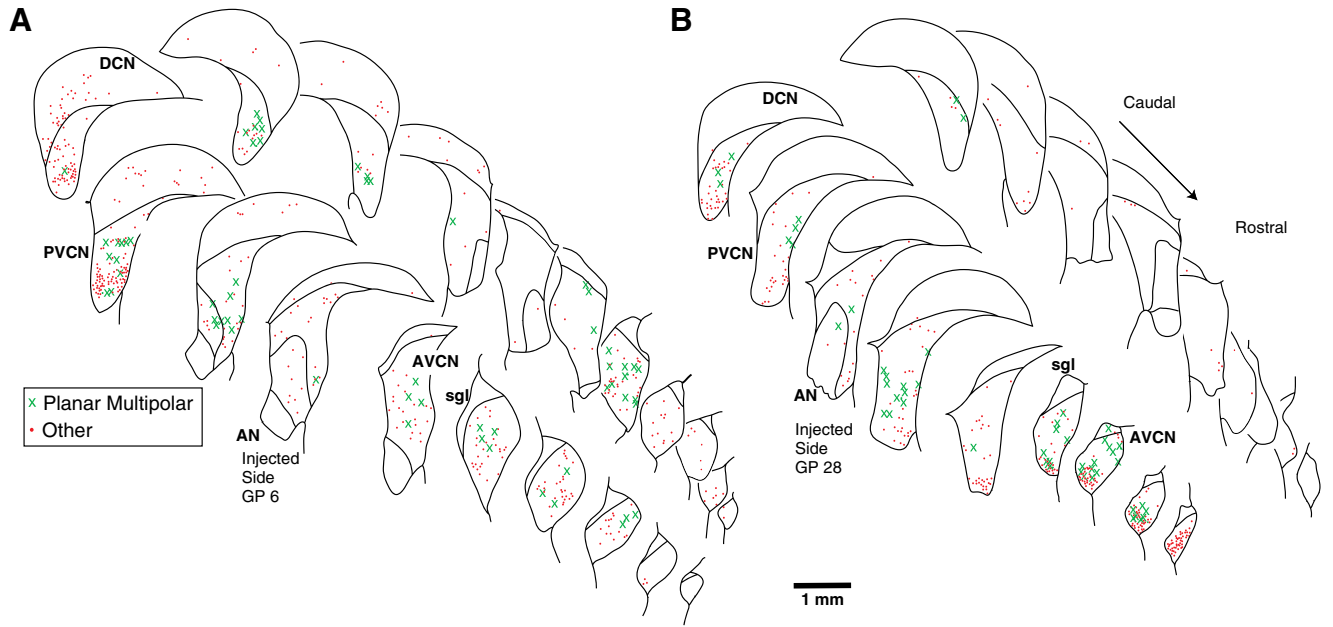
FIG. 8. Atlases showing the rostro-caudal pattern of PRV labeling in CN for two injection cases. **A** A case with abundant labeling in MOC neurons (*n*=466) and some labeling in LOC neurons (*n*=31). **B** A case with abundant labeling of both MOC neurons (*n*=172) and LOC neurons (*n*=134). Each drawing shows the superimposed labeling from four sections and each symbol represents a single labeled neuron (see key for cell type). Both the ipsilateral (injected) and contralateral sides are shown. Survival times: **A**, 4 days; **B**, 3 days. *DCN* dorsal cochlear nucleus, *PVCN* posteroventral cochlear nucleus, *AVCN* anteroventral cochlear nucleus, *AN* auditory nerve, *sgl* superficial layer of granule cells.

cells (Figs. 3A and 8A, B) usually extends through both AVCN and PVCN, although some cases had most of them in PVCN (Fig. 8A) and other cases had most of them in AVCN (Fig. 8B). Planar cells were usually found on both the ipsilateral and contralateral sides (Fig. 8A), but there were cases in which one side had more labeling of all types of cells (Fig. 8B).

Transneuronal labeling of IC disc-shaped and stellate cells

In the central nucleus of the IC, PRV labeling (Fig. 9) was observed both in neurons with disc-shaped dendritic fields and in stellate cells that have radiating dendrites as distinguished by Oliver and Morest (1984). Labeling in both types of these neurons could be as dark as OC
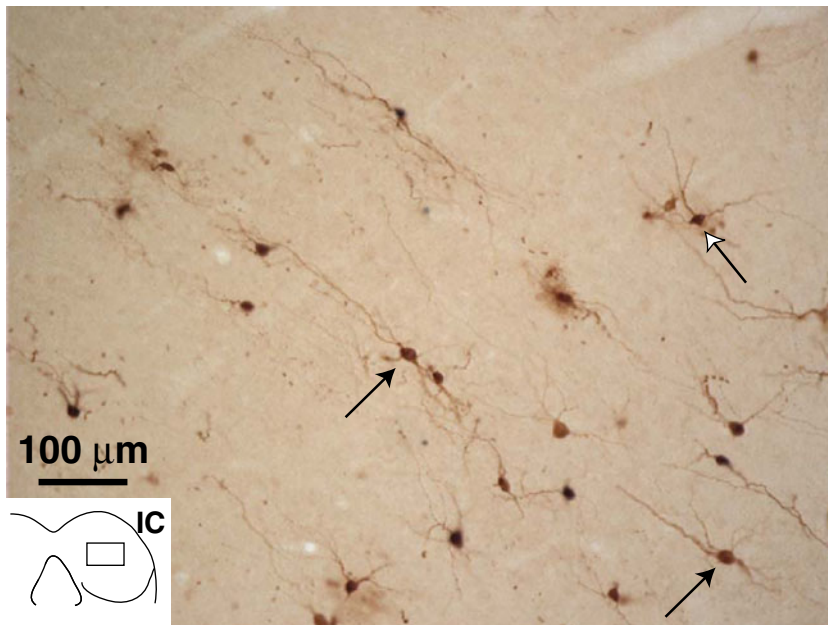

FIG. 9. Photomicrograph of PRV-labeled neurons in the IC. The dendrites of the neurons indicated by the *black arrows* have a "disc-shaped" pattern and run along the isofrequency laminae; the neuron indicated by the *white arrow* has a more radiating pattern of dendrites (stellate neuron). *Inset* shows the position of the micrograph (in the right IC, contralateral to the injection). Survival time was 4 days. This section is from the caudal IC (one quarter of the distance from the caudal-most to the rostral-most edges).
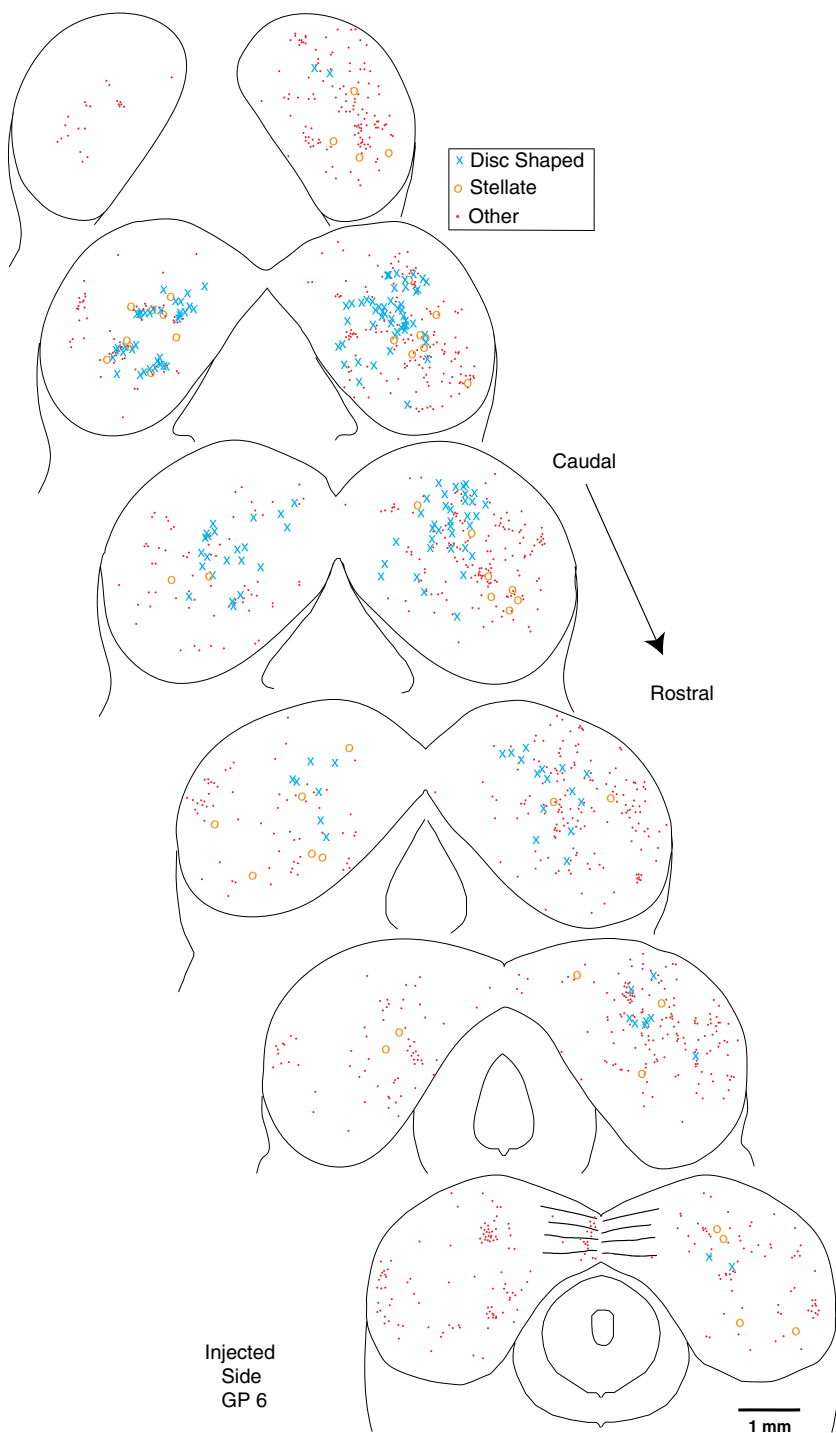
FIG. 10. Atlas showing the rostro-caudal pattern of PRV labeling in the IC for one injection case with a survival time of 4 days. This case had abundant labeling in MOC neurons and some labeling in LOC neurons (for counts, see Table 1. Each drawing shows the superimposed labeling from four sections and each symbol represents a single labeled neuron (see key for cell type).

neurons. A few neurons within each group had dendrites with numerous spines. The "disc" of the disc-shaped neurons was formed of dendrites running dorsomedially or ventrolaterally, flattened in the plane of the colliculus' fibro-dendritic laminae (Oliver et al. 1991). These dendrites extended as much as 150 μm from the soma. Cell bodies of disc-shaped neurons were small/medium in size, with 133.7 μm^2 average area (SD 39.2 μm^2, n=15 cells, average major axis 16.5 μm and

average minor axis 11.3 μm). Labeled disc-shaped cells (blue X's on Figs. 3A, B and Fig. 10) were the most numerous of the identified cells in the central nucleus. They were somewhat more concentrated in caudal sections of the central nucleus, but otherwise the rostro-caudal pattern of IC labeling was fairly uniform (Fig. 10). In cases with predominantly MOC labeling, there was abundant labeling of neurons with disc-shaped dendritic fields (blue X's in Fig. 3B and Fig. 10).
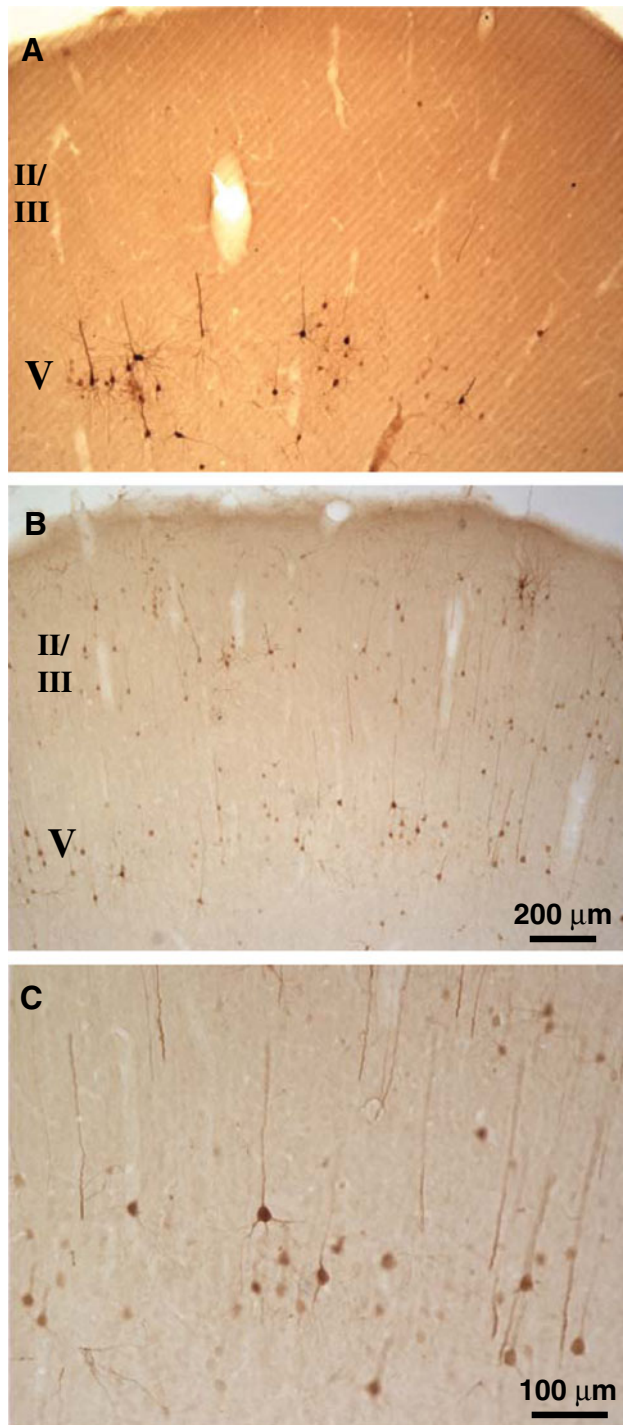
FIG. 11. Photomicrographs of PRV-labeled neurons in contralateral auditory cortex. **A** Labeling is observed mostly in pyramidal neurons of V after a 3-day survival time. **B**, **C** Labeling in layers II/III and V in a case with a 4-day survival time. These sections are about midway between the caudal and rostral edges of the auditory cortex. *Scale bar* in **B** applies to **A** and **B**.

In contrast, PRV-labeled stellate cells in the IC had radiating dendrites extending in most directions (Fig. 9). Their cell bodies ranged in size although most are large, having 224.1 µm² average area (SD

96.1 µm², n=18 cells, average major axis 29.0 µm and average minor axis 12.9 µm). The remainder of the labeling was seen in cells that could not be identified because of poor dendritic labeling or dendrites that were partially contained in other sections. Large, stellate-shaped neurons were also found in the lateral cortex of the colliculus. And elsewhere, stellate-shaped neurons were transneuronally labeled in the nuclei of the lateral lemniscus. There was more labeling in the ventral than in the dorsal nuclei of the lateral lemniscus.

Transneuronal labeling in the auditory cortex

Auditory cortex transneuronal labeling on the contra-lateral side was usually greater than that on the ipsilateral side. The labeled cortical neurons were pyramidal cells with distinct long dendrites (Fig. 11). As seen in Fig. 11A, the cells were mostly in layer V for 3-day survival times (ratio of layer V to other labeling more than 10:1 in three cases). However, for 4- and 5-day survival times (Fig. 11B, C, there was some labeling in layers II and III; ratio of layer V to other labeling averaged 1.4:1 in five of these cases). One of the cases with cortical labeling had OC neuron labeling almost exclusively in MOC neurons, suggesting that cortical transneuronal labeling could be generated via the synapses on MOC neurons. One 4-day survival case had some labeling throughout the cortex in addition to the auditory cortex. This case also had extensive labeling in the brainstem reticular formation. Our material was not optimally sectioned for observation of PRV labeling in the medial geniculate body, but neurons there were labeled in all three cases examined (survival times were 4–5 days).

Transneuronal labeling in other brainstem structures

Labeling in brainstem structures not typically associated with the auditory pathway was observed at survival times comparable to those for auditory centers (Fig. 2). Labeling was observed bilaterally in the subcoerulean nucleus, near the locus coeruleus (Fig. 12). These labeled neurons were large and multipolar. The labeling sometimes extended into the locus coeruleus. Nearby neurons in the pontine dorsal raphe were also transneuronally labeled (Fig. 12). Their medium-sized, elongated cell bodies and dendrites were vertically (dorso-ventrally) oriented along the midline of the brain. More ventrally, the pontine reticular formation had scattered bilateral labeling. Labeling here began early, at survival times of 2 days (Fig. 2A). These labeled neurons ranged from the smallest to the largest neurons that were
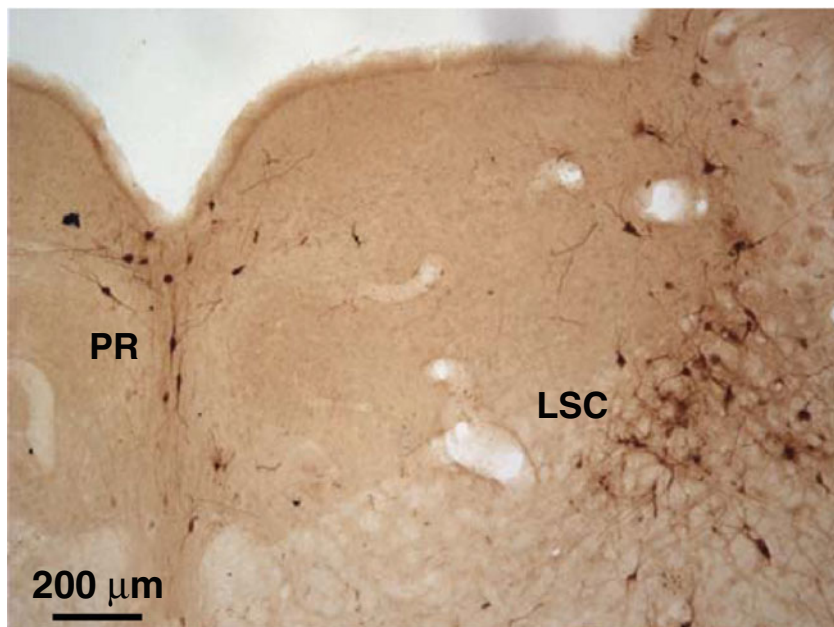
FIG. 12. Photomicrograph of labeled neurons in the pontine dorsal raphe (PR) and the locus subcoeruleus (LSC, contralateral to the injection). Survival time was 3 days. This section is just caudal to the caudal edge of the IC.

observed in this study. They had long processes extending in a variety of directions. Bilaterally, the periaqueductal gray and the dorsal tegmentum had a few transneuronally labeled neurons in less than half of our cases.

DISCUSSION

PRV transneuronal labeling of the OC pathway

A new finding of the present study is that the numbers of transneuronally labeled cells in the CN and IC are correlated with the numbers of labeled MOC neurons. We do not understand why our injection cases have differing ratios of MOC vs. LOC neurons. PRV is not known to preferentially infect certain types of neurons and our data do find both types of OC neurons labeled. Some individual variability in the ratio of LOC to MOC neurons is expected, since the ratio of unmyelinated to myelinated axons at the vestibulocochlear anastomosis has been reported (Arnesen and Osen 1984; Arnesen 1984). Additional variability in PRV labeling could be explained by injection-to-injection variation in where PRV most densely accumulates along the cochlear spiral, since most MOC neurons terminate in the base and middle portions whereas the LOC neurons terminate more evenly (Guinan et al. 1984). Variability in the MOC/LOC ratio was not pointed out by Horvath et al. (2003), although that study did not give counts for MOC neurons. They labeled more LOC neurons than the present study (560–650 vs. 0–255) and they made larger injections of PRV (50 vs. 5–30 µl). Our data do suggest

that LOC neurons are involved in transneuronal labeling to an extent, since we observed a correlation between LOC neurons and labeling in the rostral and ventral parts of the AVCN.

In both the studies of Horvath et al. (2003) and the present one, PRV labels fewer OC neurons than conventional tracers (Horvath et al. 2003; Strutz and Bielenberg 1984; Aschoff and Ostwald 1987). We found that PRV counts were only about 15 % of OC neurons labeled by other tracers. One factor in low counts may be that PRV may kill some OC neurons (e.g., Fig. 1), but this factor requires long postinoculation intervals (O'Donnell et al. 1997; Card 2001; Billig et al. 2007). Horvath et al. report a 2:1 contra/ipsi ratio of MOC neurons all of which were located in VNTB. Our ratio is closer to 1.2:1 and some MOC neurons were found in DMPO. Finally, in Horvath's study, like ours, some injections failed to produce any labeling of any OC neurons (20 % for Horvath's and 18 % for the present study). That variability was ascribed to differences of diffusion of the injection solution into the perilymph or differences in susceptibility to the PRV-Bartha among animals.

Another new finding of the present study is the identification of the particular types of cells that are transneuronally labeled in the CN (multipolar cells, especially the planar subtype) and IC (both disc-shaped and stellate neurons). Because these neurons, and neurons of the reticular formation, are labeled 1 day after the appearance of OC neuron labeling, they almost certainly provide direct input to OC neurons. Labeling at longer survival times, though, might occur via an indirect

pathway from synapses onto neurons providing direct inputs. Such secondary input might be the case for our labeling of auditory cortex and most of the "non-auditory" brainstem centers; however, a direct pathway that has a slower time course of labeling could also explain our data.

Cochlear nucleus cell types providing inputs to OC neurons

In the CN, multipolar cells are the neurons that are transneuronally labeled (Horvath et al. 2003 and present results). We found that at least half of these cells are planar cells. Projections of MOC neurons from this cell type have been shown by independent experiments using anterograde tracing of dextran amine-labeled axons (Darrow et al. 2012). The present results indicate a strong correlation between MOC labeling and PVCN transneuronal labeling. Neurons of the PVCN project to MOC neurons (Thompson and Thompson 1991) and lesions there interrupt the MOC reflex (de Venecia et al. 2005). The PVCN contains numerous planar cells (Doucet and Ryugo (1997). Thus, available data from several sources indicate that planar cells of PVCN function as the intermediate neurons of the MOC reflex. This idea fits with the fact that planar cells have dendritic fields that are narrow in the isofrequency plane of the CN (Doucet and Ryugo (1997). Their physiological correlates, "chopper units," like MOC neurons, have frequency tuning that is about as sharply tuned as auditory nerve fibers (Godfrey et al. 1975; Robertson 1984; Liberman and Brown 1986).

One major surprise from the present work is the large amount of transneuronal labeling in AVCN. There was a high correlation between MOC labeling and this labeling, suggesting that it originates from synaptic contacts with MOC neurons. Perhaps these AVCN inputs correspond to facilitatory inputs observed in physiological experiments: Most MOC neurons respond to sound in one ear (the "dominant" ear) but not to sound in the opposite ear. Stimuli in this opposite ear can, however, facilitate the unit's response to sound in the dominant ear (Liberman 1988; Brown et al. 1998). Lesion studies showing that PVCN drives the MOC response to sound (de Venecia et al. 2005) would not test these facilitatory inputs. Another possible source for some of this AVCN labeling could be LOC neurons, but this idea is not well supported by the lower correlations observed. The reason for the low transneuronal labeling via LOC neurons is not clear. It may have to do with the smaller cell bodies and thinner and shorter dendrites of these neurons (relative to MOC neurons) so that they have fewer terminals to provide a conduit for transneuronal labeling. Another possibility is that LOC neurons receive fewer inputs from higher centers like the IC

and auditory cortex. It was also surprising that we did not observe much transneuronal labeling in the superficial layer of granule cells or in the cap of small cells just below this layer. Together, these edge regions in AVCN are known as the "shell" and they are reported to contain neurons that project to OC neurons in the cat (Ye et al. 2000). Perhaps these small cells, like the small LOC neurons, are not particularly well labeled by PRV because of their size. One difference between the present results and those of Horvath et al. (2003) is that they found a slight contralateral dominance for CN labeling, whereas we found a large *ipsilateral* dominance (78.5 %). Our results fit with the finding that the MOC reflex in response to ipsilateral sound is stronger than that driven by contralateral sound and that the former proceeds via neurons in the ipsilateral CN that project to MOC neurons on the opposite side of the brainstem (Liberman and Brown 1986; Liberman and Guinan 1998).

Middle ear muscle injections of PRV yield different types of transneuronally labeled neurons. For tensor tympani injections (Billig et al. 2007), there is early labeling of large neurons with long, radiating dendrites (although longer survival times yield a wider variety of neurons). These radiate multipolar cells, some of which have been reported to project to the opposite CN (Doucet and Ryugo 2006; Brown et al. 2013b), were not labeled in the present studies. Stapedius injections of PRV yield a mixture of cell types in the CN, and labeling is seen at earlier times in the superior olivary complex (Windsor et al. 2007; Mukerji et al. 2010).

Inputs from IC

Descending inputs from IC to OC neurons were demonstrated previously by transneuronal labeling (Horvath et al. 2003), with conventional tracers (Faye-Lund 1986; Thompson and Thompson 1993; Vetter et al. 1993), and by electric stimulation (Groff and Liberman 2003; Ota et al. 2004), but the cell type of origin was not determined. The present work demonstrates transneuronal labeling in both major types of collicular neurons in the cat (Oliver and Morest 1984), neurons with disc-shaped dendritic fields and stellate neurons, which may roughly correspond to the "flat" and "less flat" types distinguished in the rat by Malmierca et al. (1993). Both of these types form ascending projections to the medial geniculate body (reviewed by Oliver and Huerta 1992). However, we do not know whether the particular cells that form ascending connections also form the descending projections labeled in the present study. The correlation between the number of MOC neurons and the number of transneuronally labeled IC neurons (Fig. 6B) suggests that here also, transneuronal labeling

proceeds mostly via MOC neurons. One difference between the present study and the work of Horvath et al. (2003) is that they found labeling confined to the central nucleus while we found a limited amount of labeling in the dorsal and lateral cortices. However, like Horvath et al. (2003), we found that the IC labeling had a slight contralateral dominance.

Inputs from the cortex and other centers

Layers V and II of the cortex are the origin of most descending projections from the cortex to lower centers (reviewed by Winer 1992). Descending inputs from pyramidal cells in layer V of the cortex to the MOC neurons have been described (Mulders and Robertson 2000a; Horvath et al. 2003). In the present study, we found transneuronal labeling in layer V, and a simple explanation for this labeling is via projections of these neurons directly to OC neurons. For the longer survival times (4 and 5 days), we also found labeling in layers II and III, but our material is not extensive enough to speculate on the pathway responsible for this labeling. Labeling in medial geniculate was also seen previously (Horvath et al. 2003).

Transneuronal labeling of the present study indicates involvement in the OC pathway of the "non-auditory" centers, such as the reticular formation (beginning at 2 days of survival time), and in the pontine dorsal raphe and the subcoerulean nucleus (beginning at 3 days of survival time). In our study, this appeared to be transneuronal labeling, since it never appeared without OC labeling. However, Horvath et al. (2003) found scattered dorsal raphe labeling at very short times after injection (1 day), sometimes *without* OC neuron labeling. We cannot explain this difference, although Horvath et al. (2003) generally used larger injection volumes, which may have been picked up by noncochlear nerve endings. Also, we found early labeling of vestibular efferent neurons, which are scattered in the dorsal pontine region (Strutz 1982) and which may have previously been counted as raphe labeling. Immunohistochemical studies show that noradrenaline-containing and serotoninergic varicosities contact both MOC and LOC neurons (Thompson and Thompson 1995; Woods and Azeredo 1999; Mulders and Robertson 2000b). The source of the serotoninergic innervation is probably the dorsal raphe and reticular neurons, and the source of the noradrenergic innervation is the locus coeruleus in the rat (Mulders and Robertson 2001) and the subcoerulean nucleus in the guinea pig (Mulders and Robertson 2005b). These non-auditory inputs represent important pathways to OC neurons, but their functional role in the reflex pathways and in hearing remains to be clarified.

REFERENCES

Arnesen AR (1984) Fibre population of the vestibulocochlear anastomosis in humans. Acta Otolaryngol 98:501–518

Arnesen AR, Osen KK (1984) Fibre spectrum of the vestibulocochlear anastomosis in the cat. Acta Otolaryngol 98:255–269

Aschoff A, Ostwald J (1987) Different origins of cochlear efferents in some bat species, rats, and guinea pigs. J Comp Neurol 264:56–72

Benson TE, Brown MC (2006) Ultrastructure of synaptic input to medial olivocochlear neurons. J Comp Neurol 499:244–257

Billig I, Yeager MS, Blikas A, Raz Y (2007) Neurons in the cochlear nuclei controlling the tensor tympani in the rat: a study using pseudorabies virus. Brain Res 1154:124–136

Brown MC, Kujawa SG, Duca ML (1998) Single olivocochlear neurons in the guinea pig: I. Binaural facilitation of responses to high-level noise. J Neurophysiol 79:3077–3087

Brown MC, de Venecia RK, Guinan JJ Jr (2003) Responses of medial olivocochlear (MOC) neurons: specifying the central pathways of the MOC reflex. Exp Brain Res 153:491–498

Brown MC, Lee DJ, Benson TE (2013a) Ultrastructure of spines and associated terminals on brainstem neurons controlling auditory input. Brain Res. doi:10.1016/j.brainres.2013.04.020.

Brown MC, Drottar M, Benson TE, Darrow KN (2013b) Commissural axons of the mouse cochlear nucleus. J Comp Neurol 521:1683–1696

Card JP (2001) Pseudorabies virus neuroinvasiveness: a window into the functional organization of the brain. Adv Virus Res 56:39–71

Card JP, Levitt P, Enquist LW (1998) Different patterns of neuronal infection after intracerebral injection of two strains of pseudorabies virus. J Virol 75:4434–4441

Contreras RJ, Gomez MM, Norgren R (1980) Central origins of cranial nerve parasympathetic neurons in the rat. J Comp Neurol 190:373–394

Darrow KN, Maison SF, Liberman MC (2006) Cochlear efferent feedback balances interaural sensitivity. Nat Neurosci 9:1474–1476

Darrow KN, Drottar M, Brown MC (2012) Planar multipolar cells in the cochlear nucleus project to medial olivocochlear neurons in mouse. J Comp Neurol 520:1365–1375

de Venecia RK, Liberman MC, Guinan JJ Jr, Brown MC (2005) Medial olivocochlear reflex interneurons are located in the posteroventral cochlear nucleus. J Comp Neurol 487:345–360

Delano P, Elgueda D, Hamame C, Robles L (2007) Selective attention to visual stimuli reduces cochlear sensitivity in chinchillas. J Neurosci 27:4146–4153

Doucet JR, Ryugo DK (1997) Projections from the ventral cochlear nucleus to the dorsal cochlear nucleus in rats. J Comp Neurol 385:245–264

Doucet JR, Ryugo DK (2006) Structural and functional classes of multipolar cells in the ventral cochlear nucleus. Anat Rec A 288A:331–344

EKSTRAND MI, ENQUIST LW, POMERANZ LE (2008) The alpha-herpes viruses: molecular pathfinders in nervous system circuits. Trends Mol Med 14:134–140

ENQUIST LW, CARD JP (2003) Recent advances in the use of neurotropic viruses for circuit analysis. Curr Opin Neurobiol 13:603–606

FAYE-LUND H (1986) Projection from the inferior colliculus to the superior olivary complex in the albino rat. Anat Embryol 175:35–52

GODFREY DA, KIANG NYS, NORRIS BE (1975) Single unit activity in the posteroventral cochlear nucleus of the cat. J Comp Neurol 162:247–268

GROFF A, LIBERMAN MC (2003) Modulation of cochlear afferent response by the lateral olivocochlear system: activation via electrical stimulation of the inferior colliculus. J Neurophysiol 90:3178–3200

GUINAN JJ JR, WARR WB, NORRIS BE (1984) Topographic organization of the olivocochlear projections from the lateral and medial zones of the superior olivary complex. J Comp Neurol 226:21–27

HACKNEY CM, OSEN KK, KOLSTON J (1990) Anatomy of the cochlear nuclear complex of the guinea pig. Anat Embryol 182:123–149

HORVATH M, RIBARI O, REPASSY G, TOTH IE, BOLDOGKOI Z, PALKOVITS M (2003) Intracochlear injection of pseudorabies virus labels descending auditory and monoaminerg projections to olivocochlear cells in guinea pig. Eur J Neurosci 18:1439–1447

HURLEY PA, CLARKE M, CROOK JM, WIS AK, SHEPHERD RK (2003) Cochlear immunochemistry—a new technique based on gelatin embedding. J Neurosci Meth 129:81–86

LIBERMAN MC (1988) Response properties of cochlear efferent neurons: monaural vs. binaural stimulation and the effects of noise. J Neurophysiol 60:1779–1798

LIBERMAN MC, BROWN MC (1986) Physiology and anatomy of single olivocochlear neurons in the cat. Hear Res 24:17–36

LIBERMAN MC, GUINAN JJ JR (1998) Feedback control of the auditory periphery: anti-masking effects of middle ear muscles vs. olivocochlear efferents. J Commun Disord 31:471–483

LOFTUS WC, MALMIERCA MS, BISHOP DC, OLIVER DL (2008) The cytoarchitecture of the inferior colliculus revisited: a common organization of the lateral cortex in rat and cat. Neuroscience 154:196–205

MALMIERCA MS, BLACKSTAD TW, OSEN KK, KARAGULLE T, MOLOWNY RL (1993) The central nucleus of the inferior colliculus in rat: a Golgi and computer reconstruction study of neuronal and laminar structure. J Comp Neurol 333:1–27

MESULAM MM (1982) Principles of horseradish peroxidase neurohistochemistry and their applications for tracing neural pathways—axonal transport, enzyme histochemistry and light microscopic analysis. In: Mesulam M-M (ed) Tracing neural connections with horseradish peroxidase. Wiley, Chichester, pp 1–151

MUKERJI S, WINDSOR AM, LEE DJ (2010) Auditory brainstem circuits that mediate the middle ear muscle reflex. Trends Amplif 14:170–191

MULDERS WHAM, ROBERTSON D (2000A) Evidence for direct cortical innervation of medial olivocochlear neurones in rats. Hear Res 144:65–72

MULDERS WHAM, ROBERTSON D (2000B) Morphological relationships of peptidergic and noradrenergic nerve terminals to olivocochlear neurones in the rat. Hear Res 144:53–64

MULDERS WHAM, ROBERTSON D (2001) Origin of the noradrenergic innervation of the superior olivary complex in the rat. J Chem Neuroanat 21:313–322

MULDERS WHAM, ROBERTSON D (2005A) Noradrenergic modulation of brainstem nuclei alters cochlear neural output. Hear Res 204:147–155

MULDERS WHAM, ROBERTSON D (2005B) Catecholaminergic innervation of guinea pig superior olivary complex. J Chem Neuroanat 30:230–242

O-DONNELL P, LAVIN A, ENQUIST LW, GRACE AA, CARD JP (1997) Interconnected parallel circuits between rat nucleus accumbens and thalamus revealed by retrograde transynaptic transport of pseudorabies virus. J Neurosci 17:2143–2167

OLIVER DL, HUERTA MF (1992) Inferior and superior colliculi. In: Webster DB, Popper AN, Fay RR (eds) The mammalian auditory pathway: neuroanatomy. Springer, New York, pp 168–221

OLIVER DL, MOREST DK (1984) The central nucleus of the inferior colliculus in the cat. J Comp Neurol 222:237–264

OLIVER DL, KUWADA S, YIN TCT, HABERLY LB, HENKEL CK (1991) Dendritic and axonal morphology of HRP-injected neurons in the inferior colliculus of the cat. J Comp Neurol 303:75–100

OSEN KK (1969) Cytoarchitecture of the cochlear nuclei in the cat. J Comp Neurol 136:453–484

OTA Y, OLIVER DL, DOLAN DF (2004) Frequency specific effects on cochlear responses during activation of the inferior colliculus in the guinea pig. J Neurophysiol 91:2185–2193

PAGANO M, GAUVREAU K (2000) Principles of biostatistics, 2nd edn. Duxbury, Pacific Grove

PICKARD GE, SMERASKI CA, TOMLINSON CC, BANFIELD BW, KAUFMAN J, WILCOX CL, ENQUIST LW, SOLLARS PJ (2002) Intravitreal injection of the attenuated Pseudorabies virus PRV Bartha in infection of the hamster suprachiasmatic nucleus only by retrograde transsynaptic transport via autonomic circuits. J Neurosci 22:2701–2710

ROBERTSON D (1984) Horseradish peroxidase injection of physiologically characterized afferent and efferent neurons in the guinea pig spiral ganglion. Hear Res 15:113–121

RYUGO DK, FAY RR, POPPER AN (2011) Auditory and vestibular efferents, vol 38. Springer, New York

SMITH BN, BANFIELD BW, SMERASKI CA, WILCOX CL, DUDEK FE, ENQUIST LW, PICKARD GE (2000) Pseudorabies virus expressing enhanced green fluorescent protein: a tool for in vitro electrophysiological analysis of transsynaptically labeled neurons in identified central nervous system circuits. Proc Natl Acad Sci USA 97:9264–9269

SPANGLER KM, HENKEL CK, MILLER IJ JR (1982) Localization of the motor neurons to the tensor tympani muscle. Neurosci Lett 32:23–27

STRUTZ J (1982) The origin of efferent innervation vestibular fibers in the guinea pig. Acta Otolaryngol 94:299–305

STRUTZ J, BIELENBERG K (1984) Efferent acoustic neurons within the lateral superior olivary nucleus of the guinea pig. Brain Res 299:174–177

THOMPSON AM, THOMPSON GC (1991) Posteroventral cochlear nucleus projections to olivocochlear neurons. J Comp Neurol 303:267–285

THOMPSON AM, THOMPSON GC (1993) Relationship of descending inferior colliculus projections to olivocochlear neurons. J Comp Neurol 335:402–412

THOMPSON AM, THOMPSON GC (1995) Light microscopic evidence of serotoninergic projections to olivocochlear neurons in the bush baby (Otolemur garnettii). Brain Res 695:263–266

VETTER DE, MUGNAINI E (1992) Distribution and dendritic features of three groups of rat olivocochlear neurons. A study with two retrograde cholera toxin tracers. Anat Embryol 185:1–16

VETTER DE, SALDANA E, MUGNAINI E (1993) Input from the inferior colliculus to medial olivocochlear neurons in the rat: a double label study with PHA-L and cholera toxin. Hear Res 70:173–186

WARR WB (1969) Fiber degeneration following lesions in the posteroventral cochlear nucleus of the cat. Exp Neurol 23:140–155

WINDSOR A, ROSKA B, BROWN MC, LEE DJ (2007) Transneuronal analysis of the middle ear muscle reflex pathways using pseudorabies virus. Abstr Assoc Res Otolaryngol, #605

WINER JA (1992) The functional architecture of the medial geniculate body and the primary auditory cortex. In: Webster DB, Popper AN, Fay RR (eds) The mammalian auditory pathway: neuroanatomy. Springer, New York, pp 222–409

WOODS CI, AZEREDO WJ (1999) Noradrenergic and serotonergic projections to the superior olive: potential for modulation of olivocochlear neuron. Brain Res 836:9–18

YE Y, MACHADO DG, KIM DO (2000) Projection of the marginal shell of the anteroventral cochlear nucleus to olivocochlear neurons in the cat. J Comp Neurol 420:127–138